Interannual Variability of Wind Power Input to near-inertial Currents in the North Atlantic

Tina Dippe, Xiaoming Zhai, Richard Greatbatch, Willi Rath

GEOMAR

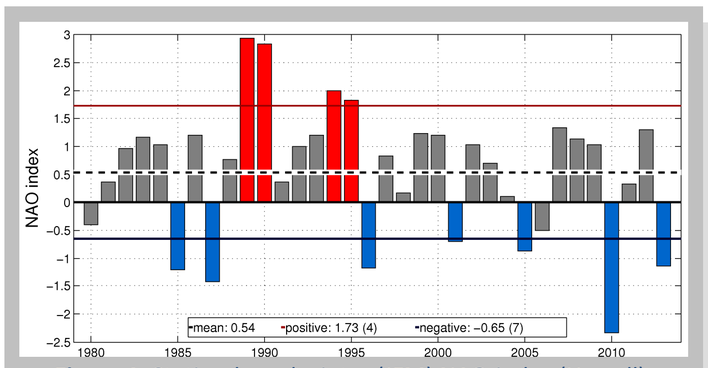

Figure 1: Station-based winter (JFM) NAO-index (Hurrell).

Why Near-Inertial Energy? – Introduction and Model

Wind Power Input (WPI) to near-inertial currents generates near-inertial energy (NIE). NIE is a source of mixing in the ocean that can affect SST[1] and has long been considered to help maintaining the MOC[2]. To investigate interannual variability of WPI, we force a high-resolution version of the MITGCM with NCEP/NCAR wind stress for the years 1989 (most positive NAO index since 1980, cf. Fig. 1) and 2010 (negative NAO).

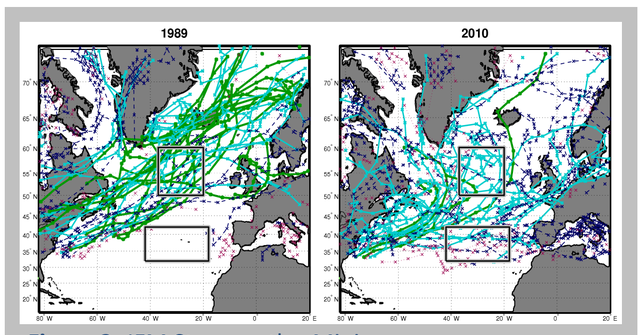

Figure 2: JFM Storm paths. Minimum core pressure: **Green**: < 960 hPa, **light blue**: < 980 hPa, **dark blue**: < 1000 hPa, **mauve**: > 1000 hPa. Boxes: cf. fig. 3.

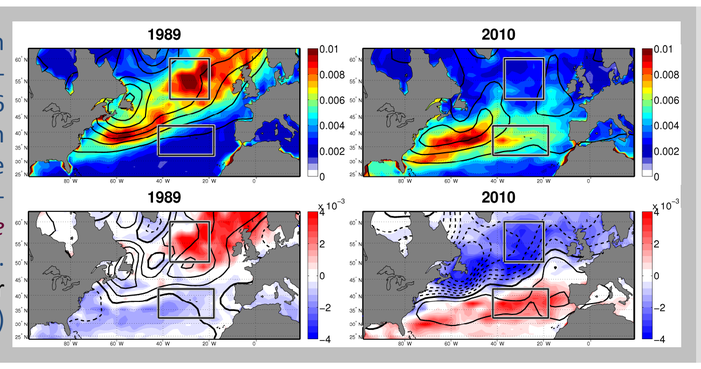

Figure 3: *Shading:* JFM mean NIWSM. Black contour lines: seasonally averaged variance of 2-6 days band-pass filtered SLP: „storm track". *Boxes*: increased WPI in the subpolar (subtropical) North Atlantic in 1989 (2010). **Top**: *Absolute values* (10 hPa² contour intervals). **Bottom**: *Anomalies* (5 hPa² contour intervals, negative values dashed)

The atmospheric conditions – NIWSM, storm paths, NAO

WPI is most efficient in response to passing storms[3]. Since a pronounced co-variability between the NAO and the North Atlantic storm track is well documented[4], we expect WPI to co-vary with the NAO. Figs. 2 and 3 illustrate the atmospheric conditions in 1989 and 2010: Individual storm paths (Fig. 2) mirror the NAO-phase. Near-inertial wind stress magnitude ("NIWSM", Fig. 3) – the part of wind stress that is most efficient in generating NIE – is related to the storm track but does not mirror it.

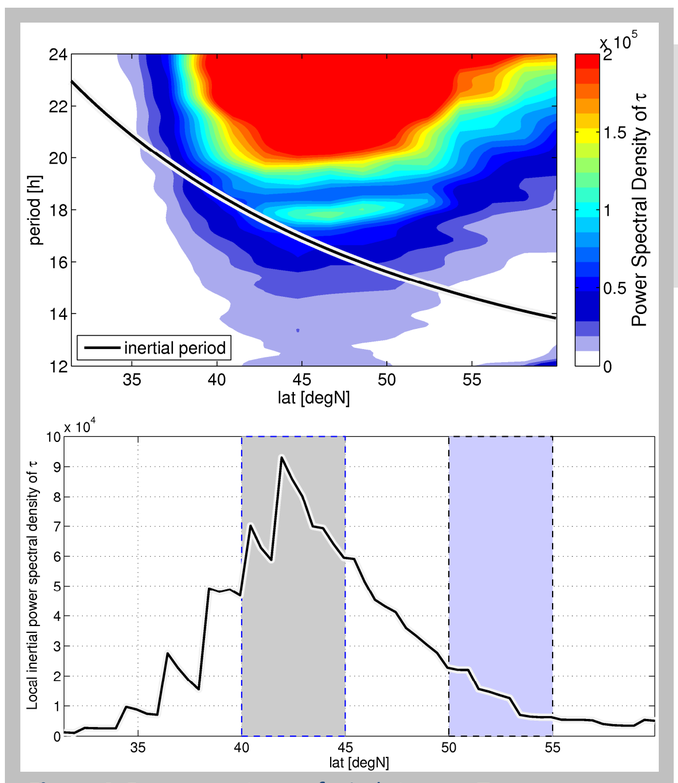

Figure 4: Power spectrum of wind stress τ. **Top**: Climatological (1980 – 2013) power spectral density (PSD) for 50°W – 40°W (shading), and local inertial frequency (black line). Raw spectra for the wind stress components were calculated separately, squared, summed and zonally averaged to yield the PSD. **Bottom**: PSD corresponding to the inertial frequency ("inertial PSD", cf. top, black line). Shaded areas correspond to the regions of enhanced climatological mean NIWSM and the core storm track (cf. fig. 3).

The Shift – Relative position of NIWSM and storm track

Fig. 3 shows that, contrary to expectations, increased NIWSM is not anchored to the storm track. This is because the variable Coriolis frequency decouples synoptic variability from near-inertial variability (Fig. 4).

Why does WPI prefer the subtropics?

Total rates of WPI in 1989 and 2010 were 8.51 and 14.51 x 10^9 W. Differences arise mainly in the subtropical and subpolar eastern North Atlantic (cf. black boxes, Fig. 5). Although mean NIWSM was comparable for these regions (Fig. 3), subtropical WPI in 2010 is enhanced. An important factor contributing to this behaviour is that positive and negative contributions to total WPI cancel each other out less effectively in the subtropics (Fig. 6).

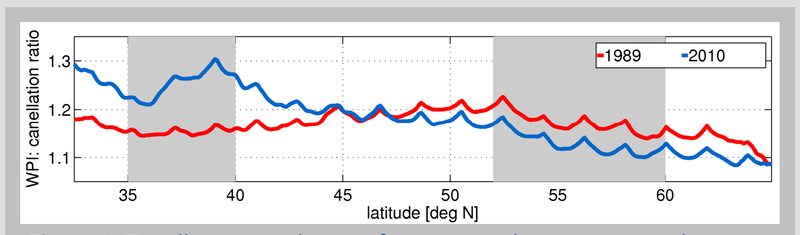

Figure 6: Zonally averaged ratio of positive and negative contributions to WPI for 40°W – 25°W ("cancellation ratio"). **Red**: 1989, **blue**: 2010. Shaded areas denote the approximate zonal region where WPI is increased in the respective year (cf. boxes figs 2, 3, 5).

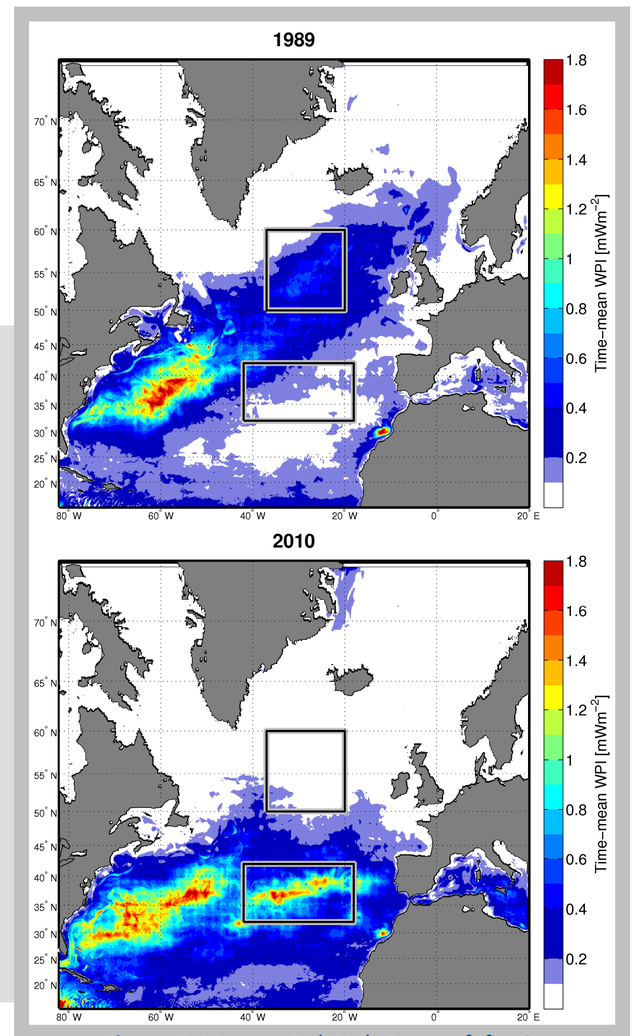

Figure 5: Mean WPI (JFM). Boxes cf. fig. 3.

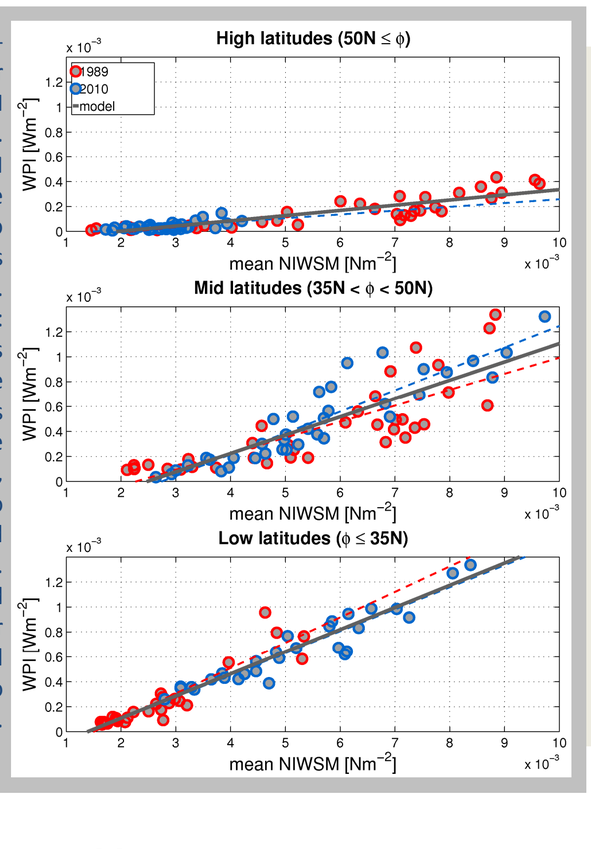

Figure 7: First-order linear regression of WPI on mean NIWSM. Both mean NIWSM and WPI data have been averaged into 5° lon x 5°lat-bins before regression. **Red**: 1989, **blue**: 2010. Dashed lines correspond to the linear models based on the respective year, solid grey lines to the model derived from both years. The combined model is used for estimating total WPI for 1980 to 2013 (Fig. 9).

Interannual Variability of WPI

To estimate past WPI, we regress it onto mean NIWSM (Fig. 7). The distribution of inertial PSD can serve as an indicator of the WPI pattern (Fig. 8). Estimates of total WPI are shown in Fig. 9. Correlations with the NAO are **-0.42**, **-0.87**, **-0.05** and **0.81** for **all**, **low**, **mid** and **high** latitudes, i.e.: Total WPI is only weakly correlated with the NAO.

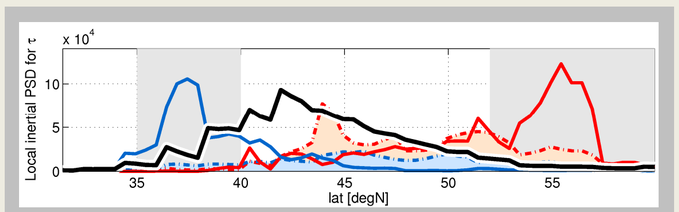

Figure 8: Inertial PSD (cf. fig. 4) of τ in the eastern Atlantic (40°W – 25°W): Indicator of the spatial distribution of WPI in dependence of the NAO phase. Solid colored (dash-dotted) lines: **blue**: 2010 (NAO- composite, cf. Fig. 1), **red**: 1989 (NAO+), **black**: climatological.

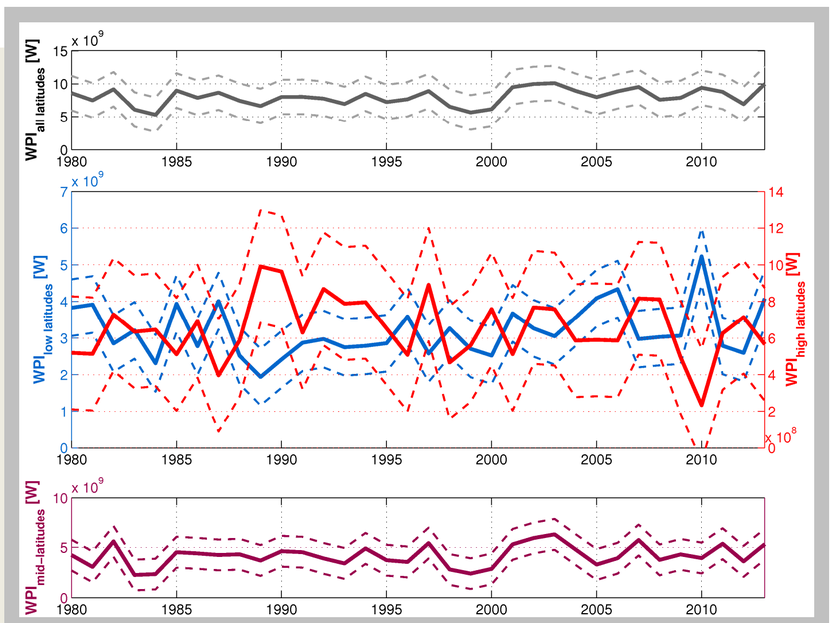

Figure 9: Time series of basinwide WPI [W] derived from mean NIWSM based on the linear model presented in Fig. 7. Top: Entire basin; middle: **blue**: low latitudes (φ < 35°N), **red**: high latitudes (φ > 50°N); bottom: mid-latitudes. RMSEs (dashed lines) were estimated via leave one out-cross validation.

[1] Jochum, M., B. Briegleb, G. Danabasoglu et al. (2013), The Impact of Near-Inertial Waves on Climate, *Journal of Climate,* 2833-2844, **[2]** Munk, W., and C. Wunsch (1998), Abyssal Recipes II: Energetics of Tidal and Wind Mixing, *Deep Sea Res. Part I,* 1977-2010 **[3]** D'Asaro, E.A. (1985), The Energy-Flux from the Wind to Near-Inertial Motions in the Mixed Layer, *Journal of Physical Oceanography*, 1043-1059 **[4]** Ulbrich, U., G. Leckebusch, J. Pinto (2009), Extra-tropical Cyclones in the present and future Climate: A Review, *Theoretical and Applied Climatology,* 117-131

University of East Anglia

HELMHOLTZ GEMEINSCHAFT